

1. Introduction

In a previous paper we presented a double diffraction system intermediated by a slit to achieve images that were perfectly symmetric and consequently depth inverted (pseudoscopics) [1] [2]. In this same system we observed the image with normal depth (orthoscopic images), in which case the observer looks at a symmetrical diffraction order of the second diffraction process [3] [4] [5]. The achieving of an image by means of white light using two bi-dimensionally-defined diffractive elements and an intermediary pinhole resulted [6] [7] [8]. Because all results were derived of symmetric situations and the enlarging of the apertures results in loosing symmetry and extension of the image point to an aberration spot, we thought that the intermediary element was fundamental. Surprisingly, we could find that there is an interesting image that results by only using two diffractive elements. Our results with two diffraction gratings are formulated in this article while the results employing two bi-dimensionally defined diffracting elements are even more interesting [10]. The remarkable fact is how the spreading of light in open space at the first diffraction can be reversed on the second diffraction process. A rough comparison with similar refractive optics imaging processes can be made with the imaging of a white-light object through a small angle prism whose dispersion is corrected by including a compensating second prism on the light path. Besides, because the second diffractive element has almost total transparency for non-diffracted light, and therefore cannot be perceived by the observer, the image generates the illusion of a ghost image, therefore, of great attractive appearance.

2. Description

The process for obtaining white-light images for no intermediated double diffraction is described in Figure 1. The element O is a point of a three-dimensional white-light object. A set of luminous rays exiting from it impinges at point x_{1n} the first diffractive grating DG1 of $2v$ lines per millimeter which is at distance z from the object and whose lines are vertical. The corresponding diffracted rays reaching the second diffractive grating DG2 a point x_{2m} , when diffracted by it, are the double-diffracted rays we consider. DG2 is located at distance Zr from DG1, has v lines per millimeter and its lines are also vertical. The image is seen by an observer or by a camera whose pupil has a diameter close to an eye's. An imaginary set of virtual rays that are the virtual prolongation of the double-diffracted rays cross at the image i , i_b being the image for a short wavelength and i_r for a large wavelength. To analyze the capacity of the second diffraction element to receive the rays diffracted by the first and to recombine them in an image that is located next to the object we start by the simple equation of a diffraction grating.

First order diffraction at the first grating follows the equation above:

$$\sin \theta_i - \sin \theta_d = 2\lambda \cdot v \quad (1)$$

Where θ_i is the angle of incidence, θ_d is the angle of diffraction where the light results deviated for diffraction, v is the spatial frequency and λ is the wavelength, a value that comprehend all the visible spectrum. Equation 1 can be expressed in terms of coordinates as:

$$\frac{x_{1n}}{\sqrt{x_{1n}^2 + z^2}} - \frac{x_{1n} - x_{2m}}{\sqrt{(x_{1n} - x_{2m})^2 + z_R^2}} = 2\lambda_n v \quad (2)$$

λ_n is the wavelength of each ray between x_{1n} and x_{2m} .

Analogously, first order diffraction at the second grating can be expressed as:

$$-\frac{x_{1n} - x_{2m}}{\sqrt{(x_{1n} - x_{2m})^2 + z_R^2}} - \frac{x_c - x_{2m}}{\sqrt{(x_c - x_{2m})^2 + z_c^2}} = -\lambda_n v \quad (3)$$

where x_c , z_c are coordinates of the observer. The exit angle for the double diffracted rays is:

$$\phi_{dn} = \arcsin\left(\frac{x_{1n}}{\sqrt{x_{1n}^2 + z^2}} - \lambda_n v\right) \quad (4)$$

3. Experimental Setup

We employed two holographic transmission gratings of the same type, with a constant spatial frequency of 540 ± 9 lines/mm for the first grating and 503 ± 8 lines/mm for the second one. The second order of the first diffraction grating and the first order of the second grating were employed to correspond with the equations. The effective area employed on each grating was approximately 60 mm x 40 mm. They were located 660 ± 5 mm apart in parallel position. Two objects were tested, one was a domestic 40 W filament lamp with its 0,5 mm wide filament vertically located, the second an extended object composed of a metal stamp whose surface was made to diffuse light by painting with aluminum paint and of ordinary letters printed on a cardboard. It was illuminated with a 50 W halogenous lamp. In both cases they were located at the distance of 425 ± 5 mm from the first grating. The observer or the camera was located at a distance of 468 ± 5 mm to the second grating and its visual line made an angle of 6.8 degrees with the normal to the gratings. A domestic video camera SONY Handycam was employed for capturing pictures of the image in a computer. The aperture of the lens was 3 mm to keep it comparable to the aperture of a observer's eye.

4. Results and Discussions

Our first experiment made the image of the filament lamp to be compared to the image that the system gives when a 1 mm wide vertical slit is located at the first grating to select the wavelength bandwidth. Figure 2 shows the photograph of the white-light image at left, and at its right-hand side the image filtered to a red bandwidth. The images at right correspond to selecting shorter wavelengths sequentially, the two first in the green color and the last to the blue color. It is interesting to notice the distinct vertical dark fringes cutting the filtered images, because they were caused by the opaque characters-which identify the voltage and power of the lamp at its glass bulb, 27 mm in front of the filament. Each ray having a different path indicates also the perspective of a beam corresponding to the portion of the gratings being traversed and the dark horizontal fringes corresponds to the different position of the lines of the opaque characters as seen from each different viewpoint. The situation has

some analogies to a previous case of imaging through a diffraction grating [9], to refraction by a prism and to the ordinary process of imaging by a lens. When considering diffraction at a grating Figure 3 we notice that the observer sees at each wavelength a different perspective of the object because he collects rays that left the object at different angles. We show our system in Figure 4 and indicates with two virtual observers $VO_>$ and $VO_<$ the position from where an observer could see a perspective of the object which corresponds to the perspectives being collected by the observer. The position of the virtual observers looking through a grating renders a scheme that is analog to the case of a prism, although with wavelength dependence inverted. But in those cases the distance at which the object is from the deviating element is not critical, while in our experience it is. Because our system makes the perspectives to converge it can be made an analogy to the action of a lens, where each portion on the aperture launches its perspective to be collected precisely in coincidence when the focusing condition is achieved. In a similar analogy, the defocusing width on the image for a point or line object is in both cases proportional to the distance from the focused position but in our case it is distinguishable as a spectral sequence of colors, making easier to measure it. If we illuminate with two or more precisely definite wavelengths, as laser lines for example, the defocusing can be sharply measured and the object needs not to be a point or a line but can be a border. Our second experiment shows the defocusing when the object is focused, 38 mm ahead of the focused position and 48 mm behind the focused position Figure 5. In a black and white photography the spectral colors cannot be noticed. Our third experiment employed the second object described above in order to show the image of an extended object. Figure 6 shows the direct photograph of the object, Figure 7 shows its image obtained after double diffraction. Figure 8 shows the image after filtering through a common absorption blue filter because some increase in sharpness can be noticed.

5. Conclusions

It was possible to obtain an image for a process that involves only double diffraction without any intermediate element. This new optical system renders images comparable to those of a thin prism but with focusing properties. Besides, it encodes depth in a way that could be useful for remote metrology.

Acknowledgements

The “Pro-Reitoria de Pós Graduação” of Campinas State University - UNICAMP is acknowledged for a BIG fellowship for Noemí I. Rodríguez Rivera.

References

- [1] Lunazzi J J, and Rivera N I, 2002 Pseudoscopic imaging in a double diffraction process with a slit, *Opt. Express* **10** 1368-1373
<http://www.opticsexpress.org/abstract.cfm?URI=OPEX-10-23-1368>
- [2] Lunazzi J J, and Rivera N I, 2003 Pseudoscopic imaging in a double diffraction process with a slit: Critical point and experimental checking, *Proc. of XXVI ENFMC SBF* Caxambu-M.G. http://www.sbf1.if.usp.br/procs/2003/R_estendido/e97.pdf
- [3] Lunazzi J J, and Rivera N I, 2004 Orthoscopic Imaging in a Double diffraction Process with Slit, *Proc. of XXVII ENFMC SBF* Poços de Caldas-MG.
- [4] Lunazzi J J, and Rivera N I, 2005 Pseudoscopic imaging in a double diffraction process with a slit: Critical point properties, submitted to *J. Opt Soc Am A* (Domo)
- [5] Lunazzi J J, and Rivera N I, 2004 Orthoscopic White-Light Imaging by Means of Two Bi-dimensional Diffracting Elements and a Pinhole *SPIE* **5622** 1469-1473
<http://bookstore.spie.org/index.cfm?fuseaction=SearchResultsPaper>
<http://bookstore.spie.org/index.cfm?fuseaction=detailpaper&cachedsearch=1&productid=591751&producttype=pdf&CFID=1568010&CFTOKEN=23535837>
- [6] Lunazzi J J, and Magalhães D, 2005 Pseudoscopic imaging in a bidimensional double diffraction process intermediated by a pinhole, submitted to *J. Opt Soc Am A* (Domo)
- [7] Lunazzi J J, and Magalhães D, 2004 Pseudoscopic white-light imaging by means of two bi-dimensional diffracting elements and a pinhole, *SPIE* **5622** 1463-1468
<http://bookstore.spie.org/index.cfm?fuseaction=detailpaper&cachedsearch=1&productid=591749&producttype=pdf&CFID=1568010&CFTOKEN=23535837>
- [8] Lunazzi J J, Rivera N I, Magalhães D, 2004 Orthoscopic and pseudoscopic white-light imaging by means of symmetrical diffractive optical elements *Proc. of Immersive Environments in: Frontiers in Optics OSA*, Rochester, Estados Unidos da América
<http://www.abstractsonline.com/viewer/viewAbstract.asp?CKey={D7AC5005-5F0D-4E14-8560-71B7C7FAAE8A}&MKey={D9465EB9-EEA3-4476-89FC-7A424B368B75}&AKey={57B06C54-08A9-4FEE-9FDE-02D441047638}&SKey={76D813F5-F0C7-4BEF-A7FF-91ACEBF36F0F}>
- [9] Lunazzi J J, 1990 Holophotography with a diffraction grating *Opt. Eng.* **29** 15-18
- [10] To be published.

Captions for illustrations

Figure 1. Scheme for the image in a double diffraction process without intermediated element.

Figure 2. Five pictures of the filament of a lamp. Left: direct white image. Others: images filtered by means of a slit.

Figure 3. Schematic exemplification of the perspective variation associated to the wavelength value.

Figure 4. Schematic example of the perspective's convergence achieved by the system.

Figure 5. Defocusing effects on object at three positions. Left: behind focused position. Center: at focused position. Right: in front of focused position.

Figure 6. Photograph of an extended object, for comparison purposes.

Figure 7. Image of an extended object.

Figure 8. Filtered image of an extended object.

Figures

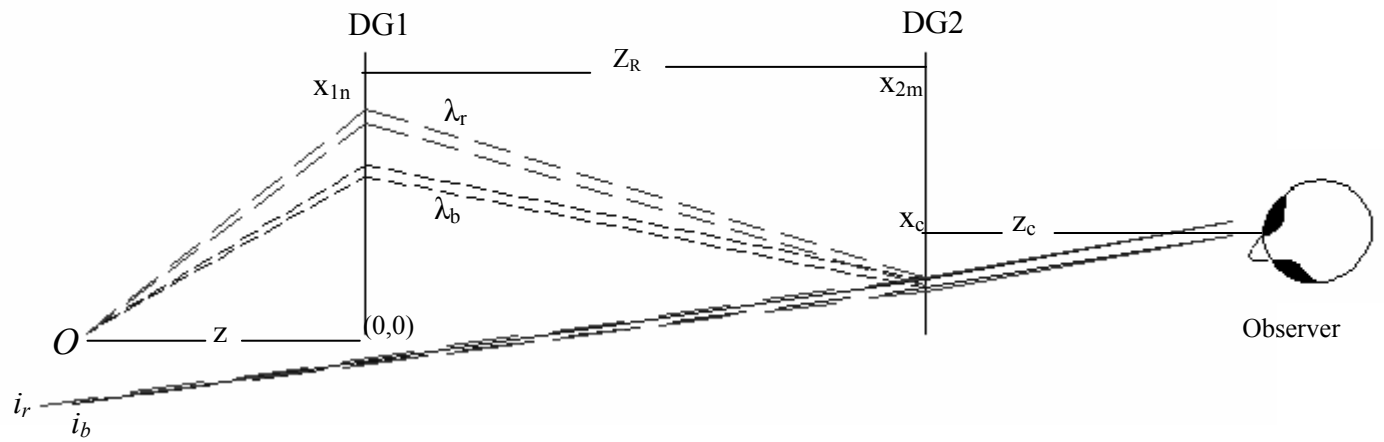


Figure 1.

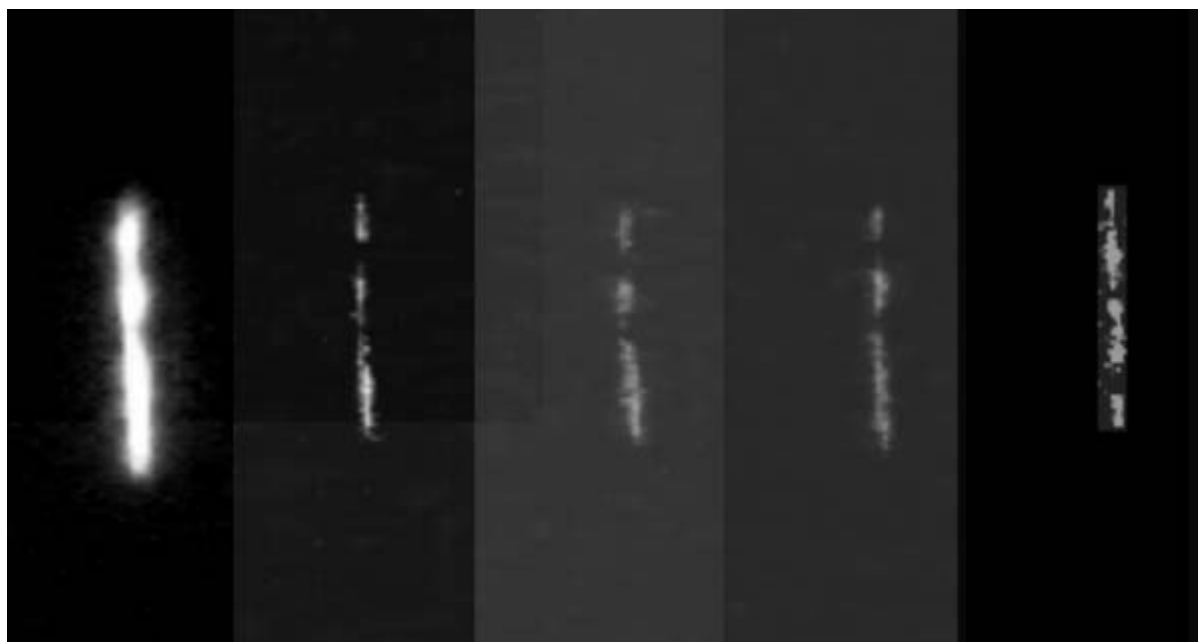


Figure 2.

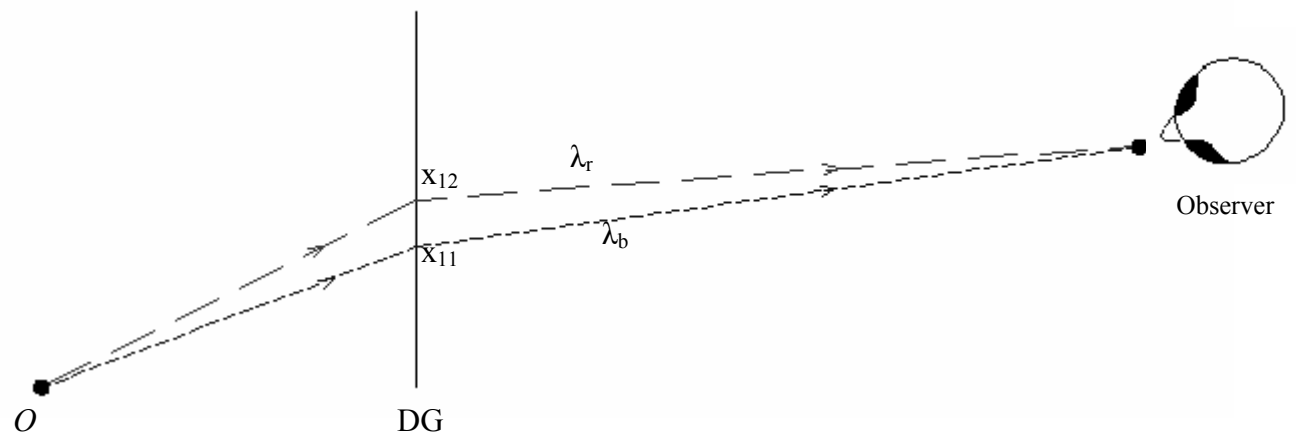


Figure 3.

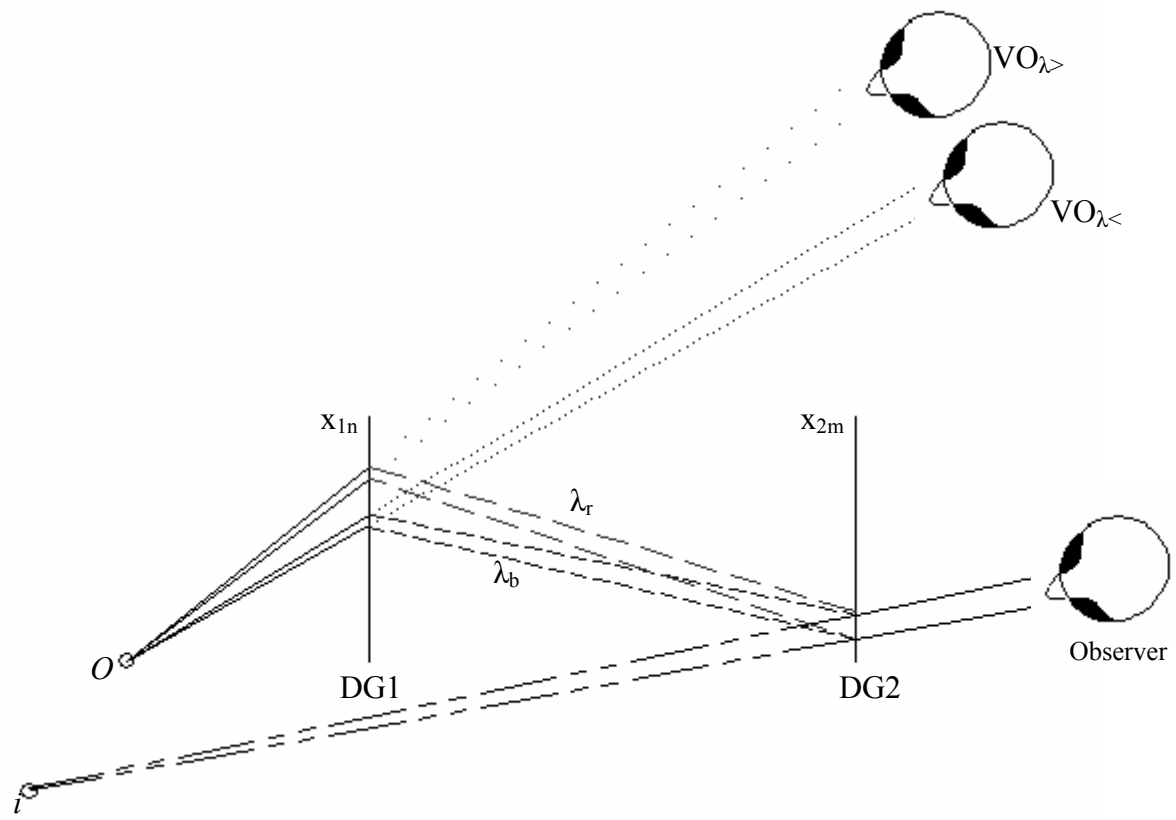


Figure 4.

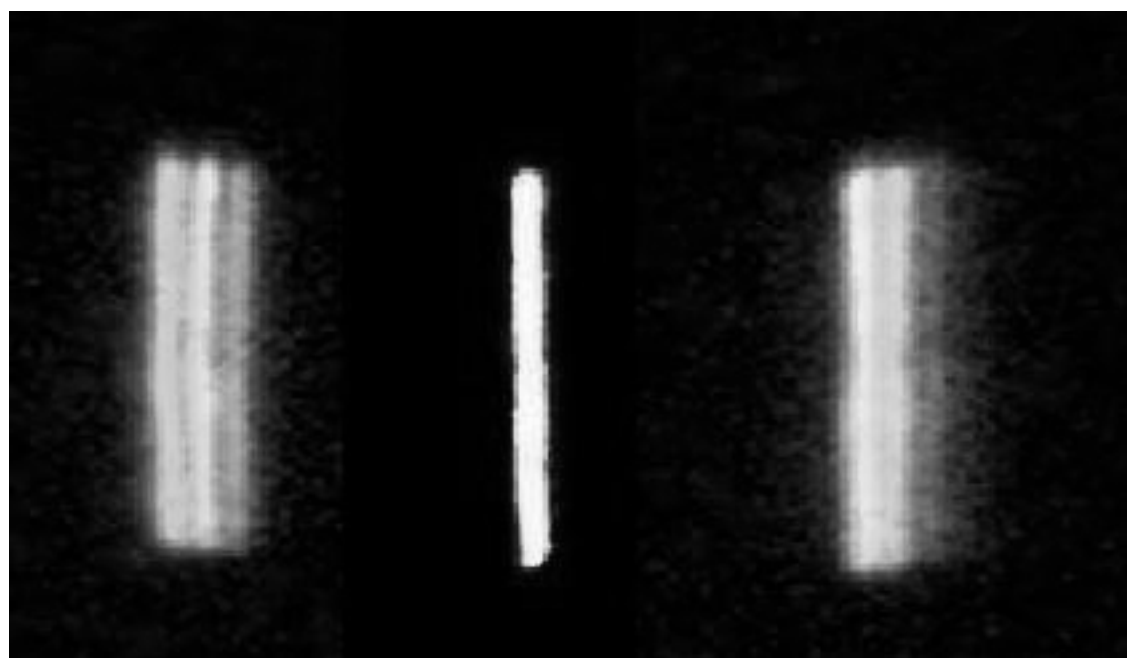


Figure 5.



Figure 6.



Figure 7.



Figure 8.